ChemPubSoc Europe

DOI: 10.1002/cctc.201500418

CHEMCATCHEM Full Papers

Highly Selective Hydrodecarbonylation of Oleic Acid into *n*-Heptadecane over a Supported Nickel/Zinc Oxide–Alumina Catalyst

Guangci Li,*[a] Feng Zhang,[a, b] Lei Chen,[a, b] Chuanhui Zhang,[a] He Huang,[a, b] and Xuebing Li*[a]

The production of second-generation biodiesel with triglycerides or their derivatives through hydroprocessing is considered as a promising approach to make transportation fuels. In this study, a series of Ni-based catalysts supported on basic composite oxides (MO-Al_2O_3, M = Mg, Ca, Ni, Cu, Zn) were prepared for the catalytic deoxygenation of oleic acid in the presence of H_2. Ni/ZnO-Al_2O_3 exhibited the highest deoxygenation activity and alkane selectivity, which depended on its moderate basicity. Investigations of the reaction conditions, which include reaction time, reaction temperature, H_2 pressure, and Ni loading, suggested that *n*-heptadecane was the predominant product and its content increased with reaction temperature. The reaction temperature was more important than H_2 pressure in the catalytic deoxygenation of oleic acid. Additionally, the overall reaction pathways for the conversion of oleic acid were proposed based on the product distribution for different durations and reaction rates of stearic acid, 1-octadecanol, and stearyl stearate, in which the oxygen atoms in the oleic acid were mainly removed in the form of CO through a hydrogenation–dehydrogenation–decarbonylation reaction route. If glycerol trioleate was used instead of oleic acid, Ni/ZnO-Al_2O_3 exhibited a high hydrodecarbonylation activity and selectivity to *n*-heptadecane.

Introduction

As a result of the conflict between the scarcity of fossil fuels and the increasing demand for transportation fuel, it is necessary to find renewable alternatives for the replacement of nonrenewable fossil resources. Vegetable oils and fats (that consist primarily of triglycerides) are promising categories for liquid transportation fuels as they are sustainable and their alkyl chains are typically in the diesel range.[1] However, crude vegetable oils and fats cannot be used directly because of their high viscosity and thermal instability. Therefore, their properties need to be upgraded to meet transportation fuel specifications.

Currently, the transesterification of vegetable oils and fats is the most popular technology to meet these requirements and involves the reaction of triglycerides with methanol into fatty acid methyl esters (FAME) and glycerol.[2] Although FAME can be mixed with petroleum-based diesel in all ratios and used directly without further modification, the low heating value and poor cold-flow properties limit its application in high-grade fuels.[3] Another technology for the production of diesel-like fuels is the deoxygenation of vegetable oils and fats (usually with hydrogenation). During this process, unsaturated bonds in the fatty-acid chains of triglycerides were saturated, meanwhile, oxygen atoms could be removed in the form of water, which leads to the increase in the energy value of the liquid products.[4] Thus, it is considered as an ideal approach for the conversion and upgrading of vegetable oil and fats into biodiesel.

The deoxygenation of triglycerides can occur through three different routes, which include hydrodeoxygenation, decarboxylation, and decarbonylation,[5] which is related closely to the reaction conditions and the catalysts. Generally, traditional sulfided transition-metal catalysts (e.g., sulfided Co-Mo and Ni-Mo) are selective for the hydrodeoxygenation route,[6] whereas supported noble-metal catalysts (e.g., Pt/Al_2O_3 and Pd/Al_2O_3) always follow decarboxylation or decarbonylation routes.[7] These catalysts are used commonly for the upgrading of vegetable oil and fats but have some shortcomings. For example, sulfided metal catalysts may cause the formation of sulfur-contaminated products, whereas noble-metal catalysts are expensive.[8] Hence, it is necessary to develop new nonsulfided metal catalysts with high activity and low cost.

In recent years, many researchers have found that supported transition metals in different forms (e.g., reduced state, oxidized state, carbides, and nitrides) exhibit high hydroprocessing activities for vegetable oil comparable to those of sulfided catalysts, and the compositions of products usually depend on

[a] Dr. G. Li,[+] F. Zhang,[+] Dr. L. Chen, C. Zhang, Dr. H. Huang, Prof. Dr. X. Li
Key Laboratory of Biofuels
Qingdao Institute of Bioenergy and Bioprocess Technology
Chinese Academy of Sciences
No.189 Songling Road, Laoshan District, Qingdao (P.R. China)
E-mail: ligc@qibebt.ac.cn
lixb@qibebt.ac.cn

[b] F. Zhang,[+] Dr. L. Chen, Dr. H. Huang
University of Chinese Academy of Sciences
No.19A Yuquan Road, Beijing (P.R. China)

[+] These authors contributed equally to this work.

Supporting Information for this article is available on the WWW under http://dx.doi.org/10.1002/cctc.201500418.

Table 1. Comparison of oleic acid conversion over Ni/MO-Al_2O_3 catalysts at 280 °C.[a]

Catalyst	Specific surface area [$m^2 g^{-1}$]	Pore volume [$cm^3 g^{-1}$]	Pore size [nm]	Conversion [%]	Distributions of liquid products [wt%]					
					n-C_{17}	*n*-C_{18}	1-Octadecanol	Stearic acid	Stearyl stearate	Stearate
Ni/MgO-Al_2O_3	153	0.29	7.6	100	23.5	3.3	5.7	1.5	–	66.0
Ni/CaO-Al_2O_3	37	0.14	12.7	100	8.3	2.4	10.3	4.8	–	74.2
Ni/NiO-Al_2O_3	116	0.42	13.3	100	93.2	2.7	–	–	–	4.1
Ni/CuO-Al_2O_3	84	0.18	5.9	100	93.8	1.3	–	–	–	4.9
Ni/ZnO-Al_2O_3	124	0.28	9.1	100	94.5	4.3	1.2	–	–	–
Ni/γ-Al_2O_3-1[b]	207	0.28	5.4	100	57.6	1.6	1.6	4.7	34.8	–
Ni/γ-Al_2O_3-2[c]	208.8	0.44	6.7	100	81.4	2.6	1.0	–	16.0	–

[a] Reaction conditions: oleic acid (2.0 g), decalin (30.0 g), 10 wt% Ni/MO-Al_2O_3 (0.2 g), H_2 pressure (3.5 MPa), and stirring at 600 rpm for 6 h. [b] The catalyst was prepared by a similar procedure to that used for the preparation of MO-Al_2O_3 supports. [c] γ-Al_2O_3 was purchased from Sasol Company.

the supports.[9] Accordingly, much attention has been paid to the effect of different supports on the conversion of vegetable oil and their model compounds. In spite of this, basic oxide supports are still mentioned rarely compared to acidic and neutral supports (e.g., zeolites, Al_2O_3, SiO_2, carbon, etc.). Basic supports can reduce the cracking of feedstock and increase the yield of liquid products; moreover, they are more favorable for the absorption of acidic fatty acids (an important intermediate derived from triglycerides) than some other supports, which may improve triglyceride deoxygenation. Herein, we synthesized several basic composite oxides (MO-Al_2O_3, M = Mg, Ca, Ni, Cu, Zn) and used them as supports for the further preparation of supported Ni/MO-Al_2O_3 catalysts. As free fatty acid is the initial hydrogenation product for triglycerides,[4b,9a–c] structurally similar oleic acid was selected as the model reactant for activity tests. Among these catalysts, Ni/ZnO-Al_2O_3 showed an excellent catalytic decarbonylation activity with the highest yield of diesel-range alkanes. To further understand the catalytic properties of Ni/ZnO-Al_2O_3, the effect of reaction conditions and the reaction pathways of oleic acid over Ni/ZnO-Al_2O_3 were investigated in detail.

Results and Discussion

Screening of supports

The XRD patterns of all as-prepared catalysts are shown in Figure 1. The diffraction peaks of elemental Ni did not appear in the patterns of most catalysts except for that of Ni/CaO-Al_2O_3, which suggests that larger Ni particles were present on the surface of Ni/CaO-Al_2O_3 because of its low surface area and the poor dispersion of Ni species. Although it is difficult to ascertain whether the surface Ni species were reduced completely into the metallic state from the XRD patterns, the change in catalyst color before and after the reduction (from yellow-green to gray or black) indicated that the reduction of surface Ni species indeed occurred. As the reduced Ni was well dispersed on various catalyst surfaces, it is concluded that their deoxygenation activities may be related closely to the composite oxide supports.

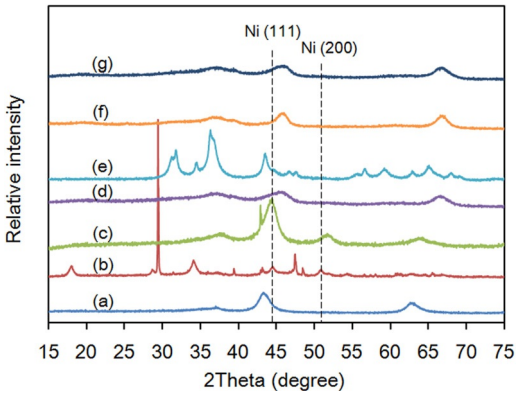

Figure 1. XRD patterns of the as-prepared catalysts: a) Ni/MgO-Al_2O_3, b) Ni/CaO-Al_2O_3, c) Ni/NiO-Al_2O_3, d) Ni/CuO-Al_2O_3, e) Ni/ZnO-Al_2O_3, f) Ni/γ-Al_2O_3-1, and g) Ni/γ-Al_2O_3-2.

Oleic acid diluted with decalin was selected as a reactant to test the catalytic deoxygenation activity of the as-prepared Ni-based catalysts, and the results are summarized in Table 1. As the double bonds of oleic acid can be saturated easily, the conversions were greater than 99%, but this does not imply that the oxygen atoms in oleic acid have been removed completely. The distributions of the liquid products derived from the various catalysts show that oleic acid can be converted into at least five substances, which include alkane, alcohol, saturated acid, ester, and salt, and their contents were dependent on the catalyst properties. The textural properties (specific surface area, pore volume, and pore size) of the catalysts differ greatly but they do not have a direct relationship with the composition of products, which indicates that these parameters are not important for oleic acid conversion under the present conditions. Thus, it is thought that chemical properties are crucial for the transformation of oleic acid. For example, if the complex oxides that contain Mg and Ca were used as supports, the corresponding products consisted mainly of stearate. It is well known that alkaline earth metal oxides, MgO and CaO, have a relatively strong basicity,[10] which favors the strong adsorption of oleic acid. Once the adsorption occurs, oleic acid may react readily to form stearate, which leads to a low yield of alkanes. With the aim to reduce the support ba-

sicity to inhibit the formation of stearate, transition metals were introduced into the supports instead of alkaline-earth metals. The results show that the content of alkanes increased markedly in association with the reduction of stearate. In particular, oleic acid was almost completely converted into alkanes over the Zn-containing support. Therefore, a support with a relatively weak basicity is favorable for the deoxygenation of oleic acid.

To further confirm the positive effect of basicity, two kinds of active alumina were used as supports to prepare the catalysts for oleic acid conversion. Although alkanes were the main product with contents of 59.2 and 84%, respectively, the selectivities were still lower for active alumina than for Ni/ZnO-Al_2O_3 (Table 1). The CO_2 temperature-programmed desorption (TPD) profiles (Figure S1) showed only one CO_2 desorption peak at 50–150 °C from Ni/γ-Al_2O_3-2, whereas an additional peak at 450–500 °C was observed for Ni/ZnO-Al_2O_3. Thus, it is reasonable to believe that a suitable basicity is favorable for the conversion of oleic acid into alkanes.

Additionally, the effect of the Ni loading on the conversion of oleic acid was studied (Figure S2). If the ZnO-Al_2O_3 support was just used as the catalyst, the conversion of oleic acid was only 7.1% and the product consisted mainly of stearyl stearate and 1-octadecanol. As the Ni loading increased to 5 wt%, a complete conversion of oleic acid was achieved, and the contents of *n*-heptadecane and *n*-octadecane were 36.2 and 3.3%, respectively. A further increase in the Ni loading resulted in a higher yield of alkanes. This phenomenon indicated that Ni species could supply the active sites for hydrogenation, which was significant for the further transformation of stearyl stearate into alkanes.

Ni/ZnO-Al_2O_3 exhibits a better catalytic deoxygenation activity than the other catalysts under identical reaction conditions (Table 1). With the purpose to investigate the structural changes of this catalyst, samples obtained at different stages of the preparation were characterized by XRD, and the corresponding patterns are shown in Figure 2. The diffraction pattern of the Zn-Al hydrate precursor is shown in Figure 2a, in which the peaks at $2\theta = 12.9$ and 26.7° can be indexed to the $Zn_4(CO_3)(OH)_6$ phase (JCPDS #11-0287). This observation is attributed to excess Zn atoms unbonded with Al atoms. The peaks at $2\theta = 31.3$, 34.4, and 36.9° are assigned to the $ZnAl_2O_4$ spinel structure (JCPDS #05-0669), which suggests that Zn-Al composite oxides can be formed directly under hydrothermal conditions. Additionally, there is a sharp peak with the strongest intensity at $2\theta = 19.5°$, however, the crystal structure cannot be determined exactly. As its position is similar to that of the (1 0 0) plane of $Zn(OH)_2$ ($2\theta = 18.9°$; JCPDS #24-1444) and it disappears after calcination (Figure 2b), this peak can probably be attributed to the $Zn(OH)_2$ phase. Moreover, the characteristic peaks of boehmite (AlOOH) were not observed, which means all Al atoms are bonded with Zn atoms through oxygen-bridged bonds to form spinel-like structures. After calcination, the Zn-Al hydrate precursor was transformed to ZnO-Al_2O_3 composite oxides, which consist mainly of $ZnAl_2O_4$ and ZnO structures (JCPDS #65-3411). Compared to $ZnAl_2O_4$, the diffraction peak intensity of ZnO is weak, which implies its smaller crystallite size.

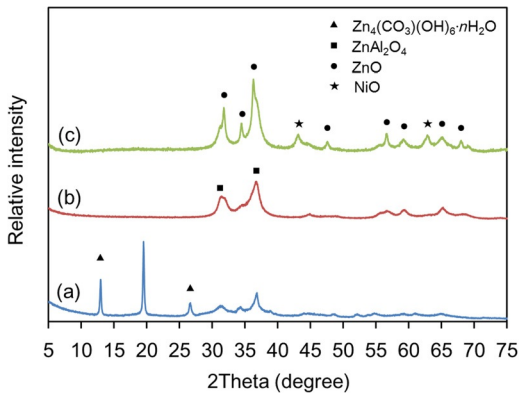

Figure 2. XRD patterns of different samples: a) Zn-Al hydrate precursor, b) ZnO-Al_2O_3 support, and c) unreduced 10 wt% Ni/ZnO-Al_2O_3.

The diffraction pattern of the unreduced Ni/ZnO-Al_2O_3 catalyst is shown in Figure 2c. Only two weak diffraction peaks were observed at $2\theta = 43.3$ and 62.8°, assigned to the (0 1 2) and (1 1 0) planes of the NiO phase (JCPDS #44-1159). Another characteristic peak of the (1 0 1) plane at $2\theta = 37.2°$ is not observed because it has a similar diffraction angle to the characteristic peak of the (3 1 1) plane of the $ZnAl_2O_4$ phase. Interestingly, the diffraction peak intensity of ZnO increases remarkably after the loading of NiO, whereas that of $ZnAl_2O_4$ remains unchanged. This reveals that the addition of NiO may promote the migration of ZnO crystallites to grow into larger particles. After reduction, the metallic Ni peak cannot be seen in the XRD pattern (Figure 1e), whereas the peaks of NiO were still observed, which indicates that only the surface NiO particles were reduced to metallic Ni under the present conditions. However, because of its trace amount and small particle size, it is difficult to detect metallic Ni by XRD. Accordingly, TEM was employed to observe the Ni particle size (Figure S3), which shows that the Ni particles were distributed uniformly on the support surface with an average size of 11.7 nm.

The effect of reaction temperature and H_2 pressure

The effect of the reaction temperature and H_2 pressure on the conversion of oleic acid was investigated to evaluate the catalytic deoxygenation performance of Ni/ZnO-Al_2O_3, and the results are listed in Table 2. As the double bonds can be saturated easily in the presence of high-pressure H_2, the conversion of oleic acid for all tests was 100% except for the reaction at 240 °C. At this temperature, stearyl stearate was the dominant product, which is attributed to an esterification reaction between the formed stearic acid and 1-octadecanol. As the temperature was increased from 240 to 280 °C, the content of alkanes increased remarkably from 0.2 to 99.2% accompanied by the reduction of the stearyl stearate content, which indicates that stearyl stearate may be an important intermediate. The alkanes in the liquid products are C_{17} and C_{18} straight-chain alkanes. Probably, because of the weak acidity of the catalyst, no isomers of C_{17} and C_{18} alkanes or their cracking products were

Table 2. Conversion of oleic acid under different temperatures and H_2 pressures.[a]

Entry	T [°C]	P [MPa]	Conversion [%]	Distributions of liquid products [wt%]			
				n-C_{17}	n-C_{18}	1-Octadecanol	Stearyl stearate
1	240	4.0	92.8	0.2	–	5.9	93.9
2	260	4.0	100	46.6	1.7	10.7	41.0
3	270	4.0	100	81.7	2.5	2.2	13.6
4	280	4.0	100	95.0	4.2	0.8	–
5	280	3.5	100	94.5	4.3	1.2	–
6	280	3.0	100	95.1	4.2	0.7	–
7	280	2.5	100	93.7	2.1	1.3	2.9[b]
8	280	2.0	100	82.3	1.6	1.2	12.9
9	280	1.0	100	59.6	0.8	0.7	38.9
10	300	2.0	100	96.2	3.8	–	–

[a] Reaction conditions: oleic acid (2.0 g), decalin (30.0 g), 10 wt% Ni/ZnO-Al_2O_3 (0.2 g), and stirring at 600 rpm for 6 h. [b] The content of zinc stearate.

detected in the products. Although the ratio of C_{17}/C_{18} decreased with the increase of the reaction temperature, C_{17} alkane (*n*-heptadecane) was still the main product.

The effect of H_2 pressure on the yield of alkanes is similar to that of temperature, that is, an increased H_2 pressure can improve the formation of alkanes, which suggests that a higher H_2 pressure is favorable for the hydrogenolysis of the intermediate (stearyl stearate) at the same reaction temperature. If the H_2 pressure was increased to 3.0 MPa, the content of alkanes was above 99%, and a further increase in the pressure did not affect the product distribution significantly.

Furthermore, if the reaction was performed at 280 °C, the selectivity to alkanes reached 60% even under a pressure of 1.0 MPa, which is much higher than that obtained at 240 °C and 4.0 MPa H_2. Thus, the reaction temperature is thought to be more critical to the conversion of oleic acid into alkanes than the H_2 pressure. To verify this assumption, a similar reaction was conducted at 300 °C and 2.0 MPa H_2. As a result, oleic acid can be transformed completely into alkanes within the same reaction time.

Conversion of oleic acid over Ni/ZnO-Al_2O_3

To investigate the transformation of oleic acid, a series of reactions were performed at 280 °C and 3.0 MPa H_2 for various reaction times from 1 to 6 h, and the results are shown in Figure 3. Within the first hour, all of the oleic acid was saturated rapidly by the hydrogenation reaction, and the primary product was stearyl stearate (78.6%) with a small amount of stearic acid (18.3%). The formation of stearyl stearate requires a large amount of 1-octadecanol in addition to stearic acid, however, only a small amount of 1-octadecanol (2.4%) was detected, which indicates that the reaction rates for the hydrogenation of oleic acid into 1-octadecanol and the esterification of 1-octadecanol with stearic acid were very fast. As the reaction progresses, the content of stearyl stearate and stearic acid decreased gradually accompanied with an increase in the content of alkanes (which include heptadecane and octadecane) and 1-octadecanol. More specifically, the increment of heptadecane is much higher than that of the other components. Heptadecane was hardly detected in the initial reaction stage even though it could be produced easily though the decarbonylation of octadecanal. These findings indicate that the formed octadecanal has been hydrogenated into 1-octadecanol and converted readily into stearyl stearate before decarbonylation. Thus, in one sense, heptadecane was derived mainly from stearyl stearate rather than oleic acid. With respect to the gas phase (data not shown), CO was the main product and its content increased as the reaction went on. Moreover, only small amounts of other products such as CO_2 and methane were observed, which suggested that catalytic decarbonylation occurred preferentially compared with direct decarboxylation over this catalyst. This is consistent with the results reported by Kandel and co-workers[11]

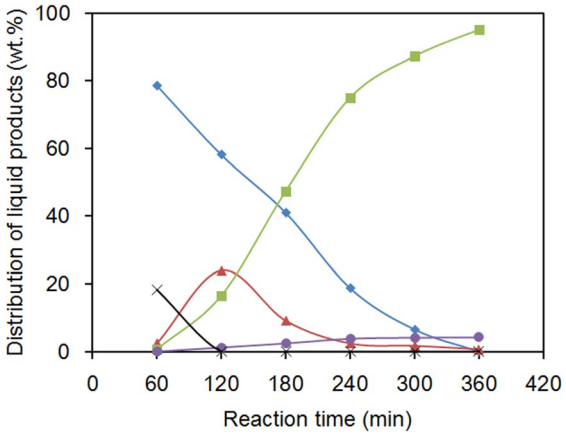

Figure 3. Distribution of liquid products for the conversion of oleic acid over 10 wt% Ni/ZnO-Al_2O_3 at 280 °C versus reaction time: (◆) stearyl stearate, (×) stearic acid, (■) *n*-heptadecane, (▲) 1-octadecanol, (●) *n*-octadecane. Reaction conditions: oleic acid (2.0 g), decalin (30.0 g), catalyst (0.2 g), H_2 pressure (3.0 MPa), and stirring at 600 rpm.

who found that the introduction of basic aminopropyl groups onto the support surface promoted decarbonylation, and heptadecane generation markedly in the hydrodeoxygenation of oleic acid. As the H_2 consumption for decarbonylation is less than that for hydrodeoxygenation, Ni/ZnO-Al_2O_3 is more economical than acidic catalysts for the production of green diesel.

Recently, Peng and co-workers found that octadecane was the dominant product in the liquid phase during the conversion of stearic acid over Ni/HBeta.[9a] Their observation is the opposite to the results in this work, which may be related to the acidy/basicity of the support used. If acidic zeolites were used as the support, the dehydration of 1-octadecanol occurred preferentially on the acid sites, which inhibited the esterification reaction with stearic acid. As a result, 1-octadecanol, as an important intermediate, was transformed mainly into octadecane. Nevertheless, basic supports cannot catalyze the dehydration of 1-octadecanol, however, they are helpful for

esterification at high temperatures.[12] Thus, a large amount of stearyl stearate was formed during the initial stage of the reaction, and *n*-heptadecane was the main finial product. Palmityl palmitate can be converted to 1-hexadecanol and hexadecanal through Ni-catalyzed hydrogenolysis.[9b] Accordingly, stearyl stearate would be transformed into 1-octadecanol and octadecanal in this work. However, only a small amount of 1-octadecanol was detected without any observation of octadecanal during the reaction, which may be because the conversion of 1-octadecnol and octadecanal is much faster than stearyl stearate hydrogenolysis. From this viewpoint, the hydrogenolysis of stearyl stearate was believed to be the rate-determining step for the overall reaction.

Kinetic experiments

For the verification of the above inferences, kinetic studies on various intermediates were performed under the same conditions (Figures S4–S6), and the corresponding initial reaction rates are shown in Table 3. As the saturation of the double bonds in oleic acid occurred easily, stearic acid would be the first intermediate. The subsequent conversion of stearic acid involves two steps: hydrogenation and esterification. If we consider that the alcohol that was esterified with stearic acid was derived from the hydrogenation of stearic acid itself then one mole of alcohol would consume one mole of stearic acid during the esterification reaction. Thus, although the conversion rate of stearic acid was calculated to be 15.4 mmol g^{-1} h^{-1} based on experimental results, the actual rate for stearic acid hydrogenation should be 7.7 mmol g^{-1} h^{-1}, which is half the conversion rate.

Table 3. Kinetic data of elementary steps in the overall deoxygenation reaction of oleic acid over 10 wt% Ni/ZnO-Al_2O_3 at 280 °C.

Elementary step	Initial rate [mmol g^{-1} h^{-1}]
Hydrogenation of stearic acid	15.4
Dehydrogenation of 1-octadecanol	9.7
Esterification of 1-octadecanol with stearic acid	64.1
Hydrogenolysis of stearyl stearate	3.3

Similar to that of stearic acid, further conversion of the generated 1-octadecanol also involved two steps: dehydrogenation and esterification. As a result of the very fast rate of the decarbonylation of 1-octadecanal, alkanes were the exclusive liquid products of the dehydrogenation of 1-octadecanol. The conversion of 1-octadecanol was linear with reaction time, and a dehydrogenation rate of 9.7 mmol g^{-1} h^{-1} was attained. In the case of the esterification reaction, the amount of solvent was doubled in the kinetics experiments to acquire a linear change of the 1-octadecanol conversion over time because the reaction rate was so fast that it was difficult to measure. In addition, the experiments were performed under N_2 to eliminate the hydrogenation reaction. Under the present conditions, the esterification rate of 1-octadecanol was calculated to be 64.1 mmol g^{-1} h^{-1}. To obtain the actual rate, a similar experiment was performed without changing the amount of solvent. As a result, the conversion of 1-octadecanol was 84.9% after 1 h, which is approximately 1.9 times as much as the present value. Thus, it is reasonable that the actual esterification rate should be 121.8 mmol g^{-1} h^{-1} if the reactant concentration remains unchanged. Apparently, the reaction rate of 1-octadecanol for esterification is much faster than that for dehydrogenation, and therefore, stearyl stearate was the predominant product in the initial stage of oleic acid conversion. Furthermore, the conversion rate of stearyl stearate was obtained from the results shown in Figure 3 and the value is 3.3 mmol g^{-1} h^{-1}, which confirms that the hydrogenolysis of stearyl stearate is the rate-determining step for the deoxygenation of oleic acid over Ni/ZnO-Al_2O_3.

If we combine these data with those reported previously by other researchers, an overall reaction pathway for the conversion of oleic acid to *n*-alkanes over Ni/ZnO-Al_2O_3 catalyst is proposed. The reaction pathway consists of six main steps that involve the saturation of C=C double bonds in the oleic acid, the hydrogenation of stearic acid, the esterification of 1-octadecanol, the hydrogenolysis of stearyl stearate, the decarbonylation of octadecanal, and the dehydrogenation of octadecanol (Scheme 1). Initially, oleic acid was hydrogenated readily into stearic acid. Then, a small amount of stearic acid may be converted into *n*-heptadecane by direct decarboxylation, and the rest was further hydrogenated into 1-octadecanol. Afterwards, most 1-octadecanol reacted with unhydrogenated stearic acid, which led to the generation of stearyl stearate, and the remainder underwent dehydration and hydrogenation with a final conversion into *n*-octadecane. Subsequently, the generated stearyl stearate was transformed into 1-octadecanol and octadecanal by hydrogenolysis. Finally, in addition to the conversion of a trace amount of 1-octadecanol into *n*-octadecane, a large proportion of 1-octadecanol was dehydrogenated into

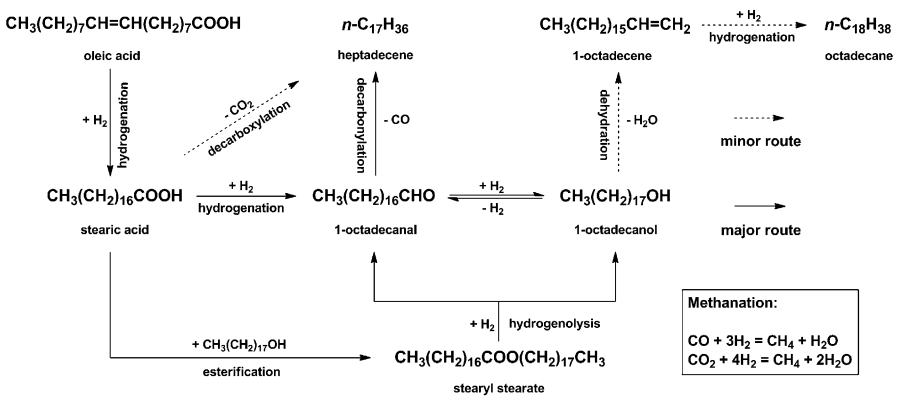

Scheme 1. Proposed reaction route for the conversion of oleic acid to alkanes over Ni/ZnO-Al_2O_3.

octadecanal and further decarbonylated into *n*-heptadecane. As the content of *n*-heptadecane is much higher than that of *n*-octadecane in the product, the decarbonylation of octadecanal is the major route compared to the hydrodeoxygenation of octadecanol. Additionally, the generated methane may derive from the reaction of the produced CO or CO_2 with H_2.

Recycling tests

The stability of the catalyst was tested under the same conditions. In each test, the recovered catalyst was recycled from the liquid product by centrifugation, washed with cyclohexane three times to remove the products, and then dried under vacuum at 60 °C for 30 min. The selectivity to alkanes decreased gradually as the number of uses increased, although oleic acid was still converted completely (Figure 4). The increment of 1-octadecanol in the product suggested that the dehydrogenation activity of the catalyst was inhibited for some reason. Recently, Song and co-workers investigated the effect of the size and distribution of Ni nanoparticles on the hydrodeoxygenation activity for microalgae oil.[13] They reported that the aggregation of Ni nanoparticles occurs during successive reactions through an Ostwald ripening process, which is a crucial factor for catalyst deactivation. In view of this, the catalyst was characterized by TEM after three runs (Figure S7), and the results show that the average size of the Ni nanoparticles had increased by over 20% (from 11.7 to 14.3 nm). As a result of the similarity of the hydrodeoxygenation reaction, the aggregation of Ni nanoparticles is believed to be the reason for the activity decrease in this work. In spite of this, the alkanes (C_{17} and C_{18}) content in the liquid product was still above 90% after three runs, which suggests a relatively high stability of the catalyst.

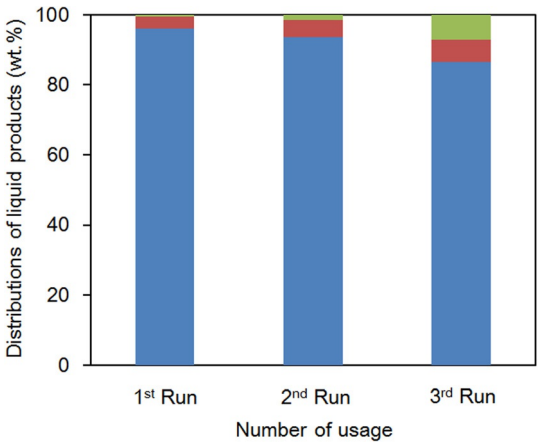

Figure 4. Recycling tests of 10 wt% Ni/ZnO-Al_2O_3 for the conversion of oleic acid: (blue) *n*-heptadecane, (red) *n*-octadecane, (green) 1-octadecanol. Reaction conditions: oleic acid (2.0 g), decalin (30.0 g), catalyst (0.2 g), temperature (280 °C), H_2 pressure (3.0 MPa), and stirring at 600 rpm for 6 h.

If we take into account that there are basic species (NiO and ZnO) on the catalyst surface, it is necessary to identify whether the oleic acid reacted with them during the reaction, which may cause the loss of active components. For this purpose, the content of Ni and Zn in the liquid product obtained from a representative reaction (performed at 280 °C and 3.0 MPa for 6 h over 10 wt% Ni/ZnO-Al_2O_3) was determined by using an Analytik Jena CONTRAA 700 atomic absorption spectrometer. Less than 1 ppm of Ni and Zn were detected, which suggests the high stability of the catalyst and that this reaction is a heterogeneous catalytic process, not catalyzed homogeneously by metals leached into the solution.

Deoxygenation reaction of triglyceride

Currently, vegetable oils are regarded as typical feedstocks for second-generation biofuels. Although triglycerides are the main component in vegetable oils, they are present as a mixture of glycerides with various unsaturated fatty-acid chains. Thus, glycerol trioleate was selected as a model compound to test the deoxygenation activity of Ni/ZnO-Al_2O_3 for triglycerides. The IR spectra of the reactant that contains glycerol trioleate and the liquid product are shown in Figure 5. The absorption peak at $\tilde{\nu} = 1748\ cm^{-1}$ in spectrum a is assigned to the stretching vibration of C=O bonds in the ester groups and the other peaks were attributed to the solvent. After the reaction, the peak at $\tilde{\nu} = 1748\ cm^{-1}$ disappeared, and a new peak at $\tilde{\nu} = 740\ cm^{-1}$ that corresponds to the rocking vibration of C–H bonds in $-CH_2-$ groups was observed in spectrum b, which means that the glycerol trioleate was converted into alkanes. This result is in accordance with that obtained from GC–MS, in which only *n*-alkanes were detected in the liquid product. The content of C_{17} alkane (94.7%) is approximately 17 times higher than that of C_{18} alkane (5.3%) in the product, which implies the high hydrodecarbonylation activity of Ni/ZnO-Al_2O_3. Compared to that of oleic acid, the conversion of glycerol trioleate needs a higher reaction temperature, and only stearyl stearate and 1-octadecanol were produced at lower temperatures (e.g., 280 °C).

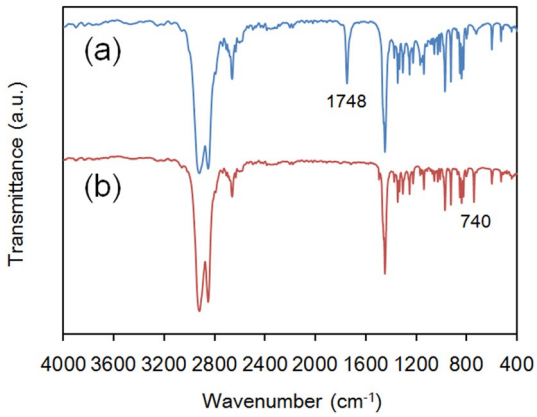

Figure 5. IR spectra of a) a decalin solution of glycerol trioleate and b) its liquid product. Reaction conditions: glycerol trioleate (2.0 g), decalin (30.0 g), 10 wt% Ni/ZnO-Al_2O_3 (0.2 g), temperature (320 °C), H_2 pressure (2.0 MPa), and stirring at 600 rpm for 6 h.

Conclusions

Various basic composite oxides were used as catalyst supports in the deoxygenation of oleic acid, and Ni supported on ZnO-Al_2O_3 exhibited the highest conversion of oleic acid and selectivity to *n*-alkanes. A suitable amount of basicity on the support is favorable for oleic acid deoxygenation. Additionally, increased Ni loadings and reaction temperatures or decreased H_2 pressures were beneficial for the formation of alkanes, especially *n*-heptadecane. As the predominant product, *n*-heptadecane was derived mainly from stearyl stearate hydrogenolysis and subsequent octadecanal decarbonylation, which is the major route in the whole reaction pathway. The reaction rates of different intermediates confirm that the hydrogenolysis of stearyl stearate is the rate-determining step for the overall reaction of oleic acid. After reuse three times, the catalyst still maintained a relatively high yield of alkanes (>90%) to show a high activity stability. As this catalyst showed a high deoxygenation activity towards oleic acid/glycerol trioleate and selectivity to alkanes, it would be a promising deoxygenation catalyst for the production of green diesel in the future.

Experimental Section

General

All chemicals were purchased from commercial suppliers and used as received without further purification: $Mg(NO_3)_2{\cdot}6H_2O$, $Ca(NO_3)_2{\cdot}4H_2O$, $Ni(NO_3)_2{\cdot}6H_2O$, $Cu(NO_3)_2{\cdot}3H_2O$, $Zn(NO_3)_2{\cdot}6H_2O$, $Al(NO_3)_3{\cdot}9H_2O$, urea, and decalin (Sinopharm, AR standard), oleic acid, stearic acid, and 1-octadecanol (Aladdin, AR standard), *n*-octadecane (Aladdin, ≥99.5% GC standard), and glycerol trioleate (Aladdin, ≥60% CP standard; the composition of the fatty acid is listed in Table S1).

Preparation of MO-Al_2O_3 supports

MO-Al_2O_3 supports were obtained from the thermal decomposition of M-Al hydrate precursors. Typically, $Mg(NO_3)_2{\cdot}6H_2O$ (4 mmol), $Al(NO_3)_3{\cdot}9H_2O$ (2 mmol), and urea (42 mmol) were dissolved in deionized water (40 mL) under magnetic stirring. The solution was transferred to a 100 mL Teflon-lined stainless autoclave and heated to 180 °C. After reaction for 3 h, the autoclave was cooled to RT, and the white precipitate was collected by filtration, washed with deionized water to get a neutral pH, and then dried in air at 80 °C overnight. Finally, the solid was calcined in air from RT to 500 °C at a heating rate of 2 °C min^{-1} and maintained for 4 h, which led to the formation of the MgO-Al_2O_3 support. Similarly, other supports were prepared with the corresponding nitrate salts by the same procedure.

Preparation of Ni/MO-Al_2O_3 catalysts

Ni/MO-Al_2O_3 catalysts were prepared by an incipient wetness impregnation method as follows: $Ni(NO_3)_2{\cdot}6H_2O$ (3.4 mmol) was dissolved in water (2.7 mL), and the solution was added dropwise onto the as-prepared MgO-Al_2O_3 support (1.8 g) with continuous agitation at RT for 2 h. Afterward, the obtained substance was dried overnight at 80 °C and then calcined in a flow of N_2 at 400 °C for 4 h (flow rate: 80 mL min^{-1}), followed by reduction at 500 °C in a flow of H_2 for 4 h (flow rate: 80 mL min^{-1}). The heating rate for calcination and reduction was 2 °C min^{-1}. The obtained sample was Ni/MgO-Al_2O_3 with 10% Ni content by weight. Similarly, other Ni supported catalysts, namely, Ni/CaO-Al_2O_3, Ni/NiO-Al_2O_3, Ni/CuO-Al_2O_3, and Ni/ZnO-Al_2O_3, were prepared by the same procedure.

Characterization

The crystal structures of the samples were analyzed by using a Bruker AXS-D8 Advance powder diffractometer with a CuK_α radiation source of wavelength 1.5406 Å. The XRD patterns were collected at 40 kV and 40 mA with a scanning rate of 4°/min from 2θ = 5–80°. The textural properties of the catalysts were obtained from N_2 adsorption–desorption isotherms measured by using a Micromeritics ASAP 2020 adsorption analyzer at −196 °C. Before the measurements, all of the samples were degassed at 140 °C under vacuum for 6 h. The specific surface areas were calculated by the BET method, and the pore volumes and pore size were determined by the Barrett–Joyner–Halenda (BJH) method from the desorption branch of the isotherms. TEM analysis was performed by using a JEM-2100HR electron microscope with an acceleration voltage of 200 kV. The reduced catalyst sample was dispersed ultrasonically in ethanol and dropped onto a carbon-coated copper grid. At least 200 Ni particles were measured to determine the Ni nanoparticle size distribution. The basicity of catalyst was analyzed by CO_2-TPD measurement by using a Micromeritics AutoChem II 2920 instrument. Before the adsorption of CO_2, the catalyst (0.1 g) was activated under Ar at 300 °C for 1 h. Then, the sample tube was cooled to 50 °C, and a mixture of 10 vol% CO_2/Ar at a flow rate of 80 mL min^{-1} was introduced into sample tube at a flow rate of 80 mL min^{-1} for 1 h. Subsequently, the sample was purged with 30 mL min^{-1} Ar at 50 °C for 2 h to remove physisorbed CO_2. Afterwards, the sample was heated to 600 °C at a rate of 10 °C min^{-1} and maintained for 20 min. The desorbed CO_2 was monitored by using a thermal conductivity detector (TCD).

Catalytic tests

Deoxygenation reactions of oleic acid were performed by using a tank reactor (100 mL capacity) with continuous stirring. Typically, oleic acid (2.0 g) was diluted with decalin (30.0 g), and the mixture was charged into the vessel, together with Ni/MO-Al_2O_3 catalyst (0.2 g). Before the reaction, the reactor was purged three times with H_2 to exchange the air inside. The reaction was performed at 280 °C and 3.5 MPa H_2 (initial pressure at RT) for 6 h with a stirring rate of 600 rpm. The products in the gas phase were analyzed by GC–MS with a TCD and an HP-PLOT/Q column (30 m, 0.32 mm inner diameter, 20 μm film). The liquid products were analyzed by GC–MS with a flame ionization detector (FID) and a HP-INNOWAX column (30 m, 0.25 mm inner diameter, 0.25 μm film). *N*-Octadecane was used as the internal standard for the quantification of the liquid products. FTIR spectra was measured by using a Nicolet 6700 spectrometer to detect the –C(O)O– group in liquid products.

Acknowledgements

This work was supported by the Qingdao Institute of Bioenergy and Bioprocess Technology Director Innovation Foundation for Young Scientists (NO. Y47203110T), and the research and development project (2014-TR-SDB-03) funded by Beijing Aeronautical

Science & Technology Research Institute of COMAC, Ltd. and Boeing Company. We also thank Dr. Y. P. Li (College of Chemical Engineering, China University of Petroleum, Qingdao, P. R. China) for TEM analysis.

Keywords: alkanes · basicity · fatty acids · nickel · supported catalysts

[1] S. A. W. Hollak, R. W. Gosselink, D. S. van Es, J. H. Bitter, *ACS Catal.* **2013**, *3*, 2837 – 2844.
[2] a) G. W. Huber, S. Iborra, A. Corma, *Chem. Rev.* **2006**, *106*, 4044 – 4098; b) E. Lotero, Y. Liu, D. E. Lopez, K. Suwannakarn, D. A. Bruce, J. G. Goodwin, *Ind. Eng. Chem. Res.* **2005**, *44*, 5353 – 5363.
[3] P. Šimáček, D. Kubička, G. Šebor, M. Pospíšil, *Fuel* **2009**, *88*, 456 – 460.
[4] a) P. Šimáček, D. Kubička, G. Šebor, M. Pospíšil, *Fuel* **2010**, *89*, 611 – 615; b) M. Fatih Demirbas, *Appl. Energy* **2009**, *86*, S151 – 161.
[5] B. Veriansyah, J. Y. Han, S. K. Kim, S. A. Hong, Y. J. Kim, J. S. Lim, Y. W. Shu, S. G. Oh, J. Kim, *Fuel* **2012**, *94*, 578 – 585.
[6] a) D. Kubička, J. Horáček, *Appl. Catal. A* **2011**, *394*, 9 – 17; b) T. M. Sankaranarayanan, M. Banu, A. Pauburangan, S. Sivasanker, *Bioresour. Technol.* **2011**, *102*, 10717 – 10723; c) O. I. Šenol, T. R. Viljava, A. O. I. Krause, *Catal. Today* **2005**, *100*, 331 – 335.
[7] a) S. Harnos, G. Onyestyák, D. Kalló, *React. Kinet. Mech. Catal.* **2012**, *106*, 99 – 111; b) A. T. Madsen, E. H. Ahmed, C. H. Christensen, R. Fehrmann, A. Riisager, *Fuel* **2011**, *90*, 3433 – 3438; c) I. Simakova, B. Rozmyslowicz, O. Simakova, P. Mäki-Arvela, A. Simakov, D. Y. Murzin, *Top. Catal.* **2011**, *54*, 460 – 466.
[8] a) O. I. Šenol, T. R. Viljava, A. O. I. Krause, *Appl. Catal. A* **2007**, *326*, 236 – 244; b) O. I. Šenol, E. Ryymin, T. Viljava, A. O. I. Krause, *J. Mol. Catal. A* **2007**, *268*, 1 – 8.
[9] a) B. Peng, Y. Yao, C. Zhao, J. A. Lercher, *Angew. Chem. Int. Ed.* **2012**, *51*, 2072 – 2075; *Angew. Chem.* **2012**, *124*, 2114 – 2117; b) B. Peng, C. Zhao, S. Kasakov, S. Foraita, J. A. Lercher, *Chem. Eur. J.* **2013**, *19*, 4732 – 4741; c) M. Krár, S. Kovács, D. Kalló, J. Hancsók, *Bioresour. Technol.* **2010**, *101*, 9287 – 9293; d) R. W. Gosselink, D. R. Stellwagen, J. H. Bitter, *Angew. Chem.* **2013**, *125*, 5193 – 5196; e) J. Han, J. Duan, P. Chen, H. Lou, X. Zheng, H. Hong, *Green Chem.* **2011**, *13*, 2561 – 2568; f) S. Lestari, P. Mäki-Arvela, I. Simakova, J. Beltramini, G. Q. Max Lu, Yu. D. Murzin, *Catal. Lett.* **2009**, *130*, 48 – 51; g) J. Monnier, H. Sulimma, A. Dalai, G. Caravaggio, *Appl. Catal. A* **2010**, *382*, 176 – 180.
[10] H. Hattori, *Chem. Rev.* **1995**, *95*, 537 – 558.
[11] K. Kandel, C. Frederickson, E. A. Smith, Y.-J. Lee, I. I. Slowing, *ACS Catal.* **2013**, *3*, 2750 – 2758.
[12] X. Meng, Q. Pan, T. Yang, *J. Am. Oil Chem. Soc.* **2011**, *88*, 143 – 149.
[13] W. Song, C. Zhao, J. A. Lercher, *Chem. Eur. J.* **2013**, *19*, 9833 – 9842.

Received: April 17, 2015
Published online on July 28, 2015